

## TEXTURING OF MULTICRYSTALLINE SILICON BY LASER ABLATION

J. Rentsch, F. Bamberg, E. Schneiderlöchner<sup>1</sup> and R. Preu  
Fraunhofer Institute for Solar Energy Systems (ISE), Heidenhofstr. 2, D-79110 Freiburg, Germany,  
email: jochen.rentsch@ise.fraunhofer.de

**ABSTRACT:** The application of laser ablation for texturing purposes represents a suitable alternative to common wet chemical texturing schemes. In this paper, a patented texturing scheme, consisting of a laser ablation step followed by plasma-chemical removal of the laser debris has been applied to conventional screen-printed multicrystalline silicon (mc-Si) solar cells. Depending on the laser parameters weighted reflectance values below 20 % are achievable with aspect ratios above 1 (depth to width). The application of the Laser-Plasma texturing scheme to conventional mc-Si solar cells results in an increase of  $j_{sc}$  of about 1 mA/cm<sup>2</sup> compared to planar etched reference cells indicating the improved optical properties. With a further adaptation of the front side screen-printed metallisation grid, significant improvements of the cell efficiency could be achieved in the future.

**Keywords:** Crystalline, Laser Processing, Texturisation

### 1 INTRODUCTION

The application of laser processing in solar cell manufacturing has gained more importance recently by the development of laser edge isolation or rear contacting schemes [1]. The suitability of laser techniques also for the texturization of crystalline silicon has been demonstrated by several groups in the past [2][3][4]. Especially for multicrystalline silicon, the reflectance reduction potential of laser textured surfaces is superior to common isotropic wet chemical etching solutions, which are limited to a minimum reflectance of approximately 20 %. Laser processing is independent of the initial surface structure, enabling effective texturisation even on very smooth or polished wafers.

Further on laser texturing offers some principal features especially for the processing of thin wafers:

- The process of laser ablation works contactless, no further mechanical stress is induced to the wafer reducing wafer breakage in the production line.
- The depth of field of a standard laser focussing unit can be chosen sufficiently deep to scribe regularly over uneven material with the same depth of texture. Steps between crystal grains will be smoother and more suitable for the screen printing technique used in standard processes.
- Patterns in the surface texture can easily be implemented without any additional masking and etching steps.
- The laser ablation step can be part of an inline processing scheme, enabling high wafer throughput and a better yield caused by less wafer handling steps.

Nevertheless the silicon surface is covered by debris after the ablation step and therefore the molten and recrystallized silicon material has to be removed in order to improve the electrical quality of the textured surface. The focus of this work lies in the investigation of the ablation process of silicon by a Nd:YAG-laser for texturing of multicrystalline silicon wafers followed by either wet or dry chemical removal of the laser induced surface damage. For the first time, a patented process sequence [5], consisting of laser texturing and plasma

removal of the laser debris has been applied to industrial type mc-Si solar cells.

### 2 EXPERIMENTAL

#### 2.1 Laser-textured sample preparation

For the optimisation of the laser texturing step different trials were made varying the wavelength, the focal length, the pulse energy and the pulse width of the scanning Nd:YAG laser system to find optimum parameters for low damage and high aspect ratios. For the dry removal of the laser debris, a microwave based plasma etching step with high etch rates and low plasma induced damage on a dynamic inline plasma etching system has been chosen [6]. A wet chemical removal of the debris has been undertaken using a short HF dip followed by KOH etching for 100 seconds for reference. The obtained surface patterns were characterised by Scanning Electron Microscopy (SEM) and reflectivity measurements. QSSPC measurements were performed on lowly doped Cz silicon (3 – 6  $\Omega$ cm) [10], to investigate the damage of the silicon after the laser texturing and plasma etching steps in reference to wet chemically planar etched and textured samples.

#### 2.1 Solar cell fabrication

The process sequence has also been adapted to conventional screen-printed mc-Si solar cells (Figure 1).

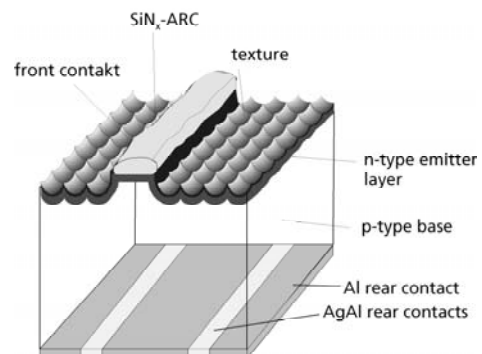


**Figure 1:** Solar cell structure with honeycomb like Laser-Plasma-textured surface.

<sup>1</sup> Present address: Deutsche Cell GmbH, Bertelsdorfer Str. 111 A, D-09599 Freiberg, Germany

The texture pattern has been adapted to the front side metallisation grid leaving out the contact areas. Following a standard industrial solar cell process, the cells have been fabricated including a  $\text{POCl}_3$  emitter diffusion ( $R_{sh} = 40 \Omega/\text{sq.}$ ), sputtered  $\text{SiN}_x$  antireflection coating [7] and aluminum back surface field (Al-BSF) at the rear side. The screen printing of the front contacts had to be aligned to the texture pattern, firing has been performed in a lamp heated RTP reactor [8] followed by an edge isolation with a Nd:YAG laser system [1].

### 3 LASER ABLATION

Pre-requisite for an effective texturing for solar application is a high aspect ratio (depth to width) with overall structure widths in the range of several micrometers. The variation of the diode current of the scanning Nd:YAG laser system revealed aspect ratios of more than 1 for a laser diode current of 38 A and a pulse energy of around 1.5 mJ (see Figure 2). The pulse length

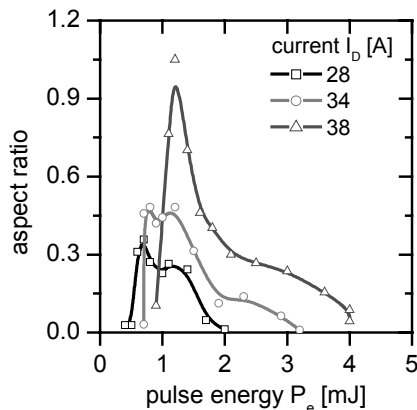


**Figure 2:** Dependence of the aspect ratio of laser textured structures from the laser pulse energy for different diode currents.

for such a process is in the range of around 150 ns. Higher pulse energies generally enforce the silicon ablation itself, also leading to an enlargement of the crater width. In contrast, the pulse length affects mainly the ablation depth due to a decreasing beam residence time.

Incomplete evaporation of silicon leads to the creation of silicon deposit, called debris, around the laser formed structure (see Figure 3, left). The deposit

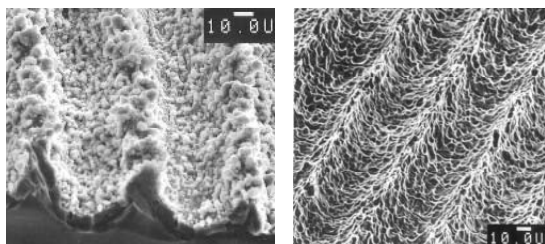


**Figure 3:** SEM picture of a laser textured surface before (left) and after (right) debris removal by plasma etching.

mainly consists of molten and recrystallized silicon and has to be removed prior to further processing. Well known is the debris removal by wet chemical etching using hydrofluoric acid (HF) and caustic potash (KOH), in this paper such an etching sequence is used for reference. Replacing the wet chemical debris removal by an anisotropic plasma etching step offers the possibility for a complete dry texturing sequence. The etching has been performed on a newly developed inline dynamic plasma etching system with a microwave-based etching sequence using  $\text{SF}_6 / \text{O}_2$  as source gas mixture. Due to the oxygen content of the etch gas mixture the overall surface structure can be preserved even though the laser induced debris is removed [9]. The resulting surface structure is shown in Figure 3 on the right side, revealing a plasma induced sub-structure due to micro-masking effects of the laser debris during etching.

### 3.2 Optical characterization

Utilizing the hatching function of the laser software a honeycomb like surface structure can be realized. Figure 4 shows a SEM top view and cross-section of such a textured surface. Minimum feature sizes of around

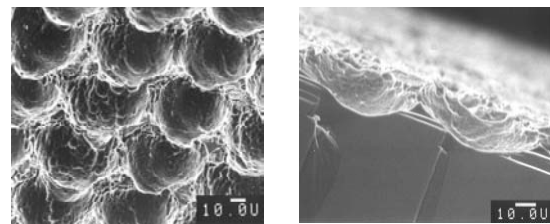


**Figure 4:** SEM top view and cross-section of a textured surface with laser ablated honeycombs (LHC).

55  $\mu\text{m}$  width and 20 to 30  $\mu\text{m}$  depth could be realized after debris removal by plasma etching. This result in reflection values (weighted from 300 to 1200 nm with the solar spectrum) of less than 20% on multicrystalline silicon (see Figure 5) with the Laser-honeycomb like surface structure (LHC). Thus, a reduction of overall reflection losses by a factor of three compared to an alkaline plain etched surface could be achieved.

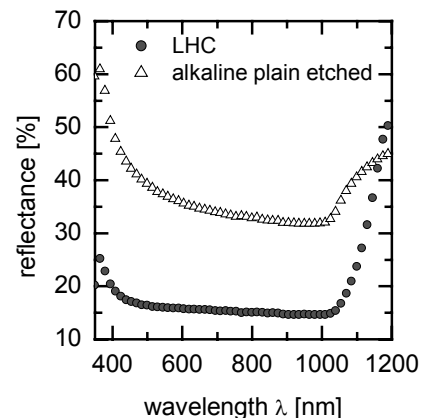


**Figure 5:** Reflectance curve of a Laser-honeycomb-texture (LHC) compared to an alkaline plain etched surface both on multicrystalline silicon.

To investigate the quality of the resulting surface structures lifetime measurements have been undertaken using the QSSPC method under low level injection on lowly doped Cz-Si wafers (3–6  $\Omega\text{cm}$ ). Wafers are prepared either with and without a  $\text{POCl}_3$  diffusion step to investigate the impact of a following high temperature treatment. Surface passivation has been carried out by depositing a hydrogen rich PECVD  $\text{SiN}_x\text{:H}$  layer.

In Figure 6, effective lifetimes of the LHC structure with further plasma debris removal is compared with an alkaline plain etched as well as a random pyramid textured surface. In both cases (with and without diffusion step), the laser-plasma treated samples show significantly lower effective lifetimes than the wet chemical references.

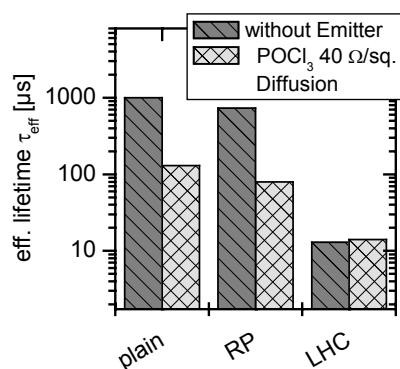


**Figure 6:** Effective lifetime of Laser-Plasma-textured surfaces compared to an alkaline etched plain and random pyramid (RP) textured surface with and without  $\text{POCl}_3$  diffusion.

#### 4 SOLAR CELL RESULTS

Solar cells have been processed on neighboring 1  $\Omega\text{cm}$  mc-Si wafers (thickness 300  $\mu\text{m}$ ) implementing the Laser-Plasma-texturing sequence. Mean as well as best cell results of the differently etched Laser features are shown in Table 1 compared to results of plasma plain etched ( $\text{SF}_6$ ) reference cells.

	$V_{oc}$ [mV]	$j_{sc}$ [mA/cm <sup>2</sup> ]	FF [%]	$\eta$ [%]
LHC	594±2	31.0±0.1	75.9±1.2	13.9±0.2
	595	31.0	78.1	14.4
LHC (wet)	595±1	31.1±0.3	76.8±1.3	14.2±0.1
	597	31.1	76.6	14.2
Reference	604±2	30.2±0.2	79.4±0.1	14.5±0.1
	605	30.3	79.5	14.6

**Table 1:** Solar cell results for Laser-Plasma-textured (LHC), Laser-textured and wet chemically etched (LHC wet) as well as Plasma chemically plain etched reference solar cells. Total cell area is 21  $\text{cm}^2$ , mean values has been taken from batches of at least 5 cells.

As a result of the textured surface, the Laser-Plasma-textured cells feature a decreased open circuit voltage of around 10 mV and a 1  $\text{mA/cm}^2$  increase in short circuit

current. Together with a lower fill factor, the efficiency of the Laser-Plasma-textured is still slightly lower than the plasma plain etched reference cells.

Evaluation of the external quantum efficiency of the best neighboring mc-Si solar cells reveals the superiority of the textured cells in terms of reflectance and light trapping properties (see Figure 7). Up to 400 nm the improved reflectance values of the textured cells increase the EQE up to 10 %, between 700 and 1000 nm the EQE

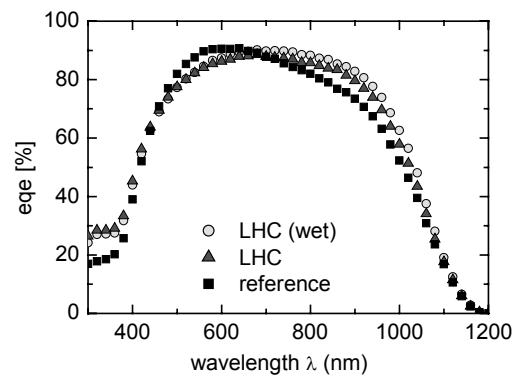


**Figure 7:** External quantum efficiencies of the Laser-textured and differently etched solar cells compared to an alkaline etched reference solar cell.

increase is even higher. This benefit may be explained by an increased light absorption near the pn-junction because the textured surface leads to shallower refraction angles. Besides the good optical performance of the cells, the lower fill factor can be mainly explained by process induced difficulties at the wafers front side. Emitter formation at the planar contact areas results in a slightly higher phosphorus diffusion leading to lower sheet resistivities. This would lead to a lower contact resistance and therefore lower series resistance, e.g. a higher fill factor. In contrast, homogeneous  $\text{SiN}_x$  deposition results in thicker layers in planar contact areas, making the firing through contacting of the screen printed metallisation grid more difficult.

An analysis of the internal quantum efficiency of the processed mc-Si solar cells is shown in Figure 8. Both textured solar cells show lower IQE's up to 700 nm, indicating a significant impact of the laser textured and etched surface at the solar cells front side. By examination of the dark characteristics and the IQE's of the processed solar cells, the exact alignment of the screen printed front contact grid seems to be one of the main challenges observed for this solar cell concept. From analysis of the dark characteristics, a nearly one order of magnitude higher saturation current of the second diode  $j_{02}$  is observed for the textured cells. Such high values can be explained by contacting textured areas with high feature sizes. Due to the significantly larger surface, emitter formation and  $\text{SiN}_x$  layer thickness is modified and therefore the firing through conditions are different to the planar contact areas. Metallisation of such areas results in deeper penetration of the screen printed contact into the silicon and therefore induces leakage currents across the pn-junction. Larger contact areas could reduce these losses accepting a slightly lower gain in short circuit current density due to a reduction of the

overall textured surface area. Besides the lower fill factor this would also explain the lower open circuit voltage of the textured solar cells.

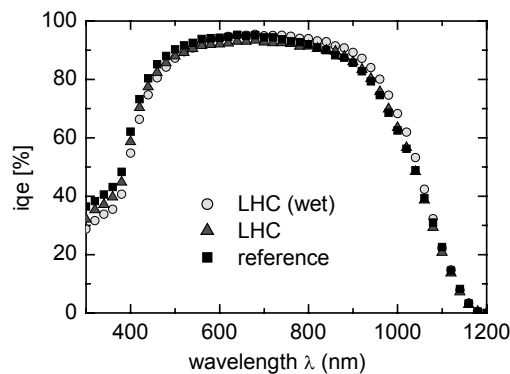


**Figure 8:** Internal quantum efficiencies of the Laser-textured and differently etched solar cells compared to an alkaline etched reference solar cell.

## 5 UPSCALING OF THE LASER PROCESS

For a homogeneous texture of a  $12.5 \times 12.5 \text{ cm}^2$  silicon wafer, more than 3 million laser ablated holes of around  $100 \mu\text{m}$  in diameter are needed. Even the used laser system with scanning optic needs more than 7 seconds per  $\text{cm}^2$  for the ablation of the honeycomb like structure therefore drastically increasing the process time. Newly developed Laser systems operating with pulse repetition rates in the MHz range could significantly accelerate the process time per  $\text{cm}^2$ . Even though, for an industrial realization of the Laser-Plasma texturing scheme many laser systems would be needed, therefore costs per Wp would increase significantly. Beam multiplication e.g. by beam dividers represent reasonable solutions for a significant reduction of process time and therewith equipment costs for an application of laser texturing processes in a future inline solar cell production line.

## 6 SUMMARY

In this paper, the potential of a Laser-Plasma texturing scheme applied to conventional mc-Si solar cells could be demonstrated. An optimization of the crucial laser parameters lead to aspect ratios in the range of 1 (depth to width) with feature sizes of around  $50 \mu\text{m}$ . Due to the laser ablation, process induced damage to the silicon could be removed efficiently by means of dry plasma etching in a newly developed dynamic inline plasma etching system. A conventional industrial solar cell process scheme has been adapted to the newly developed texturing scheme, leaving out the contact areas of the front side metallization grid. An increase in short circuit current density of nearly  $1 \text{ mA/cm}^2$  compared to planar plasma etched reference cells could be achieved clearly indicating the potential of the texturing scheme. Fill factor losses of around 3% are still limiting the overall cell performance, mainly attributed to alignment difficulties of the front side metallization. Larger contact areas could reduce these losses accepting a slightly lower

gain in short circuit current.

For the application of the Laser-Plasma texturing scheme in solar cell production lines, the laser process itself has to be accelerated to minimize costs per Wp. Possible solutions for a reduction of equipment costs are beam multipliers e.g. by beam dividers.

## 7 ACKNOWLEDGEMENTS

The author would like to thank Elisabeth Schäffer for cell measurements and Harald Lautenschlager and Norbert Kohn for technical assistance. Financial support by the German Federal Ministry for the Environment, Nature Conservation and Reactor Safety (BMU) under contract No. 329933E as well as by the companies Deutsche Cell GmbH, Roth&Rau AG and the Laserinstitut Mittweida (LIM) is gratefully acknowledged.

## References

- [1] E. Schneiderlöchner, A. Grohe, S. W. Glunz, R. Preu, and G. Willeke, Proc. 3<sup>rd</sup> World Conference on Photovoltaic Energy Conversion, Osaka, Japan (2003).
- [2] J. C. Zolper, S. Narayanan, S. R. Wenham, and M. A. Green, Applied Physics Letters 55 (1989) 2363-2365.
- [3] L. Pirozzi, U. B. Veterella, M. Falconieri, and E. Salza, Material Science Forum 173-174 (1995) 319-324.
- [4] M. Abbott, L. Mai, and J. Cotter, Proc. 14<sup>th</sup> International Photovoltaic Science and Engineering Conference, Bangkok, Thailand (2004).
- [5] J. Rentsch, E. Schneiderlöchner, and R. Preu, Deutsches Patent No. DE103 52 423, Fraunhofer Gesellschaft, Deutschland, (2005).
- [6] J. Rentsch, G. Emanuel, C. Schetter, T. Aumann, D. Theirich, J. Gentischer, K. Roth, M. Fritzsche, K.-H. Dittrich, and R. Preu, Proc. 3<sup>rd</sup> World Conference on Photovoltaic Energy Conversion, Osaka, Japan (2003).
- [7] W. Wolke, R. Preu, S. Wieder, and M. Ruske, Proc. of the 19<sup>th</sup> European Photovoltaic Solar Energy Conference, Paris, France (2004).
- [8] D. M. Huljic, D. Biro, R. Preu, C. Craff Castillo, and R. Lüdemann, Proc. 28<sup>th</sup> IEEE Photovoltaic Specialists Conference, Anchorage, Alaska, USA (2000) 379-382.
- [9] J. Rentsch, F. Bamberg, K. Roth, S. Peters, R. Lüdemann, and R. Preu, Proc. 31<sup>st</sup> IEEE Photovoltaic Specialists Conference, Orlando, USA (2005) in print.
- [10] R. A. Sinton, A. Cuevas, and M. Stuckings, Proc. 25<sup>th</sup> IEEE Photovoltaic Specialists Conference, Washington DC, USA (1996) 457-460.